



Published in final edited form as:

*J Immunol.* 2011 February 1; 186(3): 1747–1754. doi:10.4049/jimmunol.1001328.

## Interleukin-1 alpha modulates neutrophil recruitment in chronic inflammation induced by hydrocarbon oil<sup>1</sup>

Pui Y. Lee<sup>†,\*</sup>, Yutaro Kumagai<sup>‡,\*</sup>, Yuan Xu<sup>†</sup>, Yi Li<sup>†</sup>, Tolga Barker<sup>†</sup>, Chao Liu<sup>†</sup>, Eric S. Sobel<sup>†</sup>, Osamu Takeuchi<sup>‡</sup>, Shizuo Akira<sup>‡</sup>, Minoru Satoh<sup>‡,§</sup>, and WestleyH. Reeves<sup>†,§</sup>

<sup>†</sup>Division of Rheumatology & Clinical Immunology and Center for Autoimmune Disease, University of Florida, Gainesville, FL 32610-0221

<sup>‡</sup>Laboratory of Host Defense, WPI Immunology Frontier Research Center, Osaka University, 3-1 Yamada-oka, Suita, Osaka 565-0871, Japan

<sup>§</sup>Department of Pathology, Immunology and Laboratory Medicine, University of Florida, Gainesville, FL 32610

### Abstract

Exposure to naturally-occurring hydrocarbon oils is associated with the development of chronic inflammation and a wide spectrum of pathological findings in humans and animal models. The mechanism underlying the unremitting inflammatory response to hydrocarbons remains largely unclear. The medium-length alkane 2,6,10,14 tetramethylpentadecane (TMPD; also known as pristane) is a hydrocarbon that potently elicits chronic peritonitis characterized by persistent infiltration of neutrophils and monocytes. In this study, we reveal the essential role of interleukin (IL)-1 $\alpha$  in sustaining the chronic recruitment of neutrophils following TMPD treatment. IL-1 $\alpha$  and IL-1 receptor signaling promote the migration of neutrophils to the peritoneal cavity in a CXC chemokine receptor-2 (CXCR2)-dependent manner. This mechanism is at least partially dependent on the production of the neutrophil chemoattractant CXCL5. Moreover, although chronic infiltration of inflammatory monocytes is dependent on a different pathway requiring Toll-like receptor (TLR)-7, type-I interferon receptor, and CC-chemokine receptor-2 (CCR2), the adaptor molecules MyD88, IRAK-4, IRAK1 and IRAK2 are shared in regulating the recruitment of both monocytes and neutrophils. Taken together, our findings uncover an IL-1 $\alpha$ -dependent mechanism of neutrophil recruitment in hydrocarbon-induced peritonitis and illustrate the interactions of innate immune pathways in chronic inflammation.

### Introduction

Chronic inflammation is characterized by unremitting immune responses to persistent microbial infection or chemical agents (1). Continued influx of leukocytes and local production of inflammatory mediators are common features at sites of chronic inflammation. Although chemokine gradients play a prominent role in leukocyte migration, the mechanisms responsible for the sustained chemokine production and subsequent influx of neutrophils and monocytes in chronic inflammation are not well defined.

<sup>1</sup>This work was supported by grant R01-AR44731 from the US Public Health Service, a grant from the Lupus Research Institute, and by generous gifts from Lupus Link, Inc. (Daytona Beach, FL) and Mr. Lewis M. Schott to the UF Center for Autoimmune Disease. P.Y.L. was an NIH T32 trainee (DK07518).

Correspondence to: Westley Reeves MD, Division of Rheumatology & Clinical Immunology, University of Florida, PO Box 100221, Gainesville, FL 32610-0221, Phone: 352-273-7886; Fax: 352-846-1858, whreeves@ufl.edu.

\*These authors contributed equally to this work

Exposure to naturally-occurring hydrocarbon oils is associated with the development of chronic inflammation and a variety of pathological findings in humans and animal models (2–5). Due to their ability to enhance and sustain inflammation, hydrocarbons are often utilized as adjuvants in vaccines (6, 7). Among the most potent hydrocarbons in eliciting chronic inflammation is the medium-length alkane 2,6,10,14 tetramethylpentadecane (TMPD; also known as pristane). A single intraperitoneal dose of TMPD elicits infiltration of neutrophils and monocytes into the peritoneal cavity for several months (8). The chronic inflammatory response promotes the formation of plasmacytomas and lipogranulomas, a form of ectopic lymphoid tissue (5, 9). Depending on the genetic background, persistent inflammation in TMPD-treated mice also promotes the development of a plethora of autoimmune manifestations including autoantibodies, glomerulonephritis, arthritis, and pulmonary vasculitis (9–13). In addition, TMPD augments monoclonal antibody production by hybridoma cells by stimulating IL-6 production (14).

Recent studies have begun to unravel the mechanisms responsible for the chronic inflammation induced by TMPD. The response to TMPD is orchestrated by major components of the innate immune system. The continued influx of Ly6C<sup>hi</sup> “inflammatory” monocytes to the peritoneal cavity requires the presence of type-I interferon (IFN-I) production downstream of Toll-like receptor (TLR)-7 signaling (15). IFN-I activates the production of the monocyte chemoattractants CCL2, CCL7 and CCL12, which collectively recruit monocytes to the site of inflammation in a CC-chemokine receptor 2 (CCR2)-dependent manner (16). The persistent infiltration of neutrophils, on the other hand, remains largely unexplained. In this study, we aimed to define the mechanism of neutrophil recruitment in TMPD-induced chronic inflammation.

## Materials and Methods

### Mice

These studies were approved by the Institutional Animal Care and Use Committee. Wild-type C57BL/6, TNF- $\alpha$ <sup>-/-</sup>, CCR2<sup>-/-</sup> and IL-1R<sup>-/-</sup> mice (all on a C57BL/6 background), BALB/c, CXCR2<sup>-/-</sup> (BALB/c background), C3H/HeJ, C3H/HeOuJ, and CBA/CaJ mice were from Jackson Laboratories (Bar Harbor, ME). FcR $\gamma$ -chain<sup>-/-</sup> mice were from Taconic (Hudson, NY) and 129/Sv mice were from B&K Universal Limited (Grimston, Aldbrough, England). Mice were maintained in a specific pathogen free (SPF) facility at the Malcolm Randall VA Medical (Gainesville, FL). MyD88<sup>-/-</sup>, ASC<sup>-/-</sup>, Nalp3<sup>-/-</sup>, caspase-1<sup>-/-</sup>, IRAK-1<sup>-/-</sup>, IRAK-2<sup>-/-</sup>, IRAK-1<sup>-/-</sup> IRAK-2<sup>-/-</sup>, IRAK-4<sup>-/-</sup>, and IRF-7<sup>-/-</sup> mice (on a C57BL/6 background) and littermate controls were bred and maintained in a SPF facility at Osaka University. Mice (8–10-weeks-old) received 0.5 mL intraperitoneal (i.p.) injection of TMPD, pentadecane, n-hexadecane, squalene (Sigma-Aldrich, St. Louis, MO), or mineral oil (Harris Teeter, Matthews, NC). Peripheral blood and peritoneal exudate cells (PECs) were isolated as described (9). For morphological analysis, neutrophils were sorted using phycoerythrin (PE)-conjugated anti-Ly6G and magnetic bead-conjugated anti-PE antibodies (17). Fifty thousand sorted cells were cytocentrifuged onto glass slides (Fisher Scientific, Pittsburgh, PA) and stained using the Hema3 kit (Fisher). For IL-1 $\alpha$  and CXCL5 blockade, mice treated with TMPD for 2 weeks were given 200  $\mu$ g of anti-IL-1 $\alpha$  neutralizing antibodies, hamster IgG (Biolegend, San Diego, CA), anti-CXCL5 neutralizing antibodies or rat IgG1 isotype control antibodies (R&D Systems, Minneapolis, MN) i.p. and analysis was performed after 24 hrs.

### Real-time quantitative PCR (Q-PCR)

Q-PCR was performed as previously described (17). Briefly, total RNA was extracted from 10<sup>6</sup> peritoneal cells using Trizol (Invitrogen, Carlsbad, CA) and cDNA was synthesized

using Superscript II First-Strand Synthesis Kit (Invitrogen). Q-PCR was performed using the SYBR Green JumpStart Kit (Sigma) with an Opticon II thermocycler (Bio-Rad, Hercules, CA). Amplification conditions were: 95°C for 10 min, followed by 45 cycles of 94°C for 15 s, 60°C for 25 s, and 72°C for 25 s. After the final extension (72°C for 10 min), a melting-curve analysis was performed to ensure specificity of the products. Gene expression was normalized to 18S RNA, and expression relative to the sample with the lowest expression was calculated using the  $2^{-\Delta\Delta C_t}$  method (18). Primers used in this study were all described previously (15, 16) except for CXCL2 (Forward: AAGTTTGCCTTGACCCTGAA; Reverse: CGAGGCACATCAGGTACGAT) and CXCL3 (Forward: CCACTCTCAAGGATGGTCAA; Reverse: GGATGGATCGCTTTTCTCTG).

### Flow cytometry

The following conjugated antibodies were used: anti-CD11b-PE, anti-CD8-allophycocyanin (APC), anti-CD4-fluorescein isothiocyanate (FITC), anti-CD11c-PE, anti-B220-APCCy5.5, anti-Ly6G-PE, anti-Ly6C-FITC, anti-Ly6C-biotin, anti-Siglec F-biotin (all from BD Bioscience, San Jose, CA), anti-CCR3-Alexa 647, anti-CD11b-Pacific Blue (Biolegend), and avidin-APC (eBioscience, San Diego, CA). Cells were then stained with an optimized amount of primary antibodies or the appropriate isotype control for 10 min at room temperature as previously described (15). Fifty thousand events per sample were acquired using a CYAN ADP flow cytometer (Beckman Coulter, Hialeah, FL) and analyzed with FCS Express 3 (De Novo Software, Ontario, Canada).

### ELISA

CXCL1, CXCL2 (Peprotech, Rocky Hill, NJ) and CXCL5 ELISA (R&D Systems) were performed following the manufacturer's instructions. Optical density was converted to concentration using standard curves based on recombinant chemokines analyzed by a four-parameter logistic equation (Softmax Pro 4.3; Molecular Devices Corporation, Sunnyvale, CA).

### Cell culture

NIH3T3 cells were cultured in complete DMEM (containing 10% fetal bovine serum, 10 mM HEPES, glutamine, penicillin/streptomycin and 10 U/ml heparin) and seeded on 24 well cell-culture plates ( $10^5$  cells/well). Cells were stimulated with PBS or 500 pg/mL of recombinant IL-1 $\alpha$  (Biolegend), IL-1 $\beta$  (BD Bioscience), or IFN- $\beta$  (PBL Laboratories, Piscataway, NJ) and incubated at 37° C in a 5% CO<sub>2</sub> atmosphere for 6h. RNA extraction and QPCR were performed as described above.

### Statistical analysis

For quantitative variables, differences between groups were analyzed by the unpaired Student's t-test. Data are presented as mean  $\pm$  SE. All tests were two-sided. A p-value less than 0.05 was considered significant. Statistical analyses were performed using Prism 4.0 (GraphPad Software, San Diego, CA).

## Results

### Chronic recruitment of neutrophils induced by TMPD and other hydrocarbons

The inflammatory response to TPMD is characterized by chronic accumulation of monocytes and neutrophils in the peritoneal cavity (8). To better understand the mechanism of neutrophil recruitment in this model, we first studied the time course of neutrophil accumulation. In untreated or PBS-treated wild-type C57BL/6 mice, very few neutrophils (characterized by surface expression of the myeloid marker CD11b and the neutrophil-

specific marker Ly6G) were present in the peritoneal cavity (Figure 1A). Neutrophils begin to accumulate within 24 h of TMPD treatment, comprising about one-third of the peritoneal exudate cells (PECs; Figure 1A). The absolute number of neutrophils peaked after 2 weeks and remained stable for 4 to 6 weeks before a gradual decline was observed (Figure 1B and data not shown). Magnetic bead sorting of PECs using antibodies to Ly6G yielded polymorphonuclear cells morphologically consistent with neutrophils (Figure 1C). Based on these findings, all subsequent analyses were performed two weeks after TMPD treatment. Nevertheless, neutrophils were detectable up to 6 months post-TMPD treatment (Figure 1A, B), illustrating the chronicity of the inflammatory response. The infiltration of eosinophils, which are distinguished from neutrophils by morphology and surface expression of CCR3 and Siglec-f (19), was minimal in TMPD-treated mice (supplemental Figure 1).

In addition, an expansion of the neutrophil compartment in the peripheral blood also was evident following TMPD treatment. Whereas small numbers of inflammatory monocytes displaying high surface expression of Ly6C and no expression of Ly6G were seen in the peripheral blood of untreated mice (Figure 1D, ovals), larger numbers of neutrophils expressing intermediate levels of Ly6C (boxes) in addition to Ly6G were present. Two weeks after TMPD injection, the proportions of both Ly6C<sup>hi</sup> monocytes and neutrophils in the peripheral blood were increased by 2–3-fold compared to baseline levels (Figure 1D).

These changes were not strain specific as neutrophil influx was also detected in other wild-type strains injected with TMPD, although the greatest effect was seen in BALB/c mice (Table 1). Furthermore, we extended our analysis to other naturally-occurring hydrocarbons including mineral oil, squalene, pentadecane, and n-hexadecane. Similar to TMPD, all of these hydrocarbons elicited chronic recruitment of neutrophils into the peritoneal cavity (Figure 1E). This number of neutrophils in PECs two weeks after mineral oil or squalene treatment was similar to TMPD, whereas hexadecane or pentadecane treatment elicited slightly greater levels of neutrophils.

### TMPD-induced neutrophil recruitment is mediated by IL-1R signaling

The mechanism of hydrocarbon-induced chronic neutrophil recruitment remains unclear and appears independent of the pathways required for monocyte migration. Recent studies demonstrated that while TLR-7, IFN-I receptor, and CCR2 are essential for the persistent recruitment of Ly6C<sup>hi</sup> monocytes into the peritoneal cavity following TMPD treatment, these components are all dispensable for the neutrophil response (15, 16). To identify the mechanism(s) responsible for the chronic neutrophil influx, we first examined the role of several pro-inflammatory mediators previously implicated in the immune response to TMPD (9, 10, 17, 20). Compared to wild-type controls, mice deficient in TNF- $\alpha$  or Fc receptor  $\gamma$  chain all showed comparable levels of neutrophil recruitment two weeks after TMPD injection. The response was also similar in C3H/HeJ mice, suggesting that endotoxin is not responsible for our observations (Figure 2A). Moreover, the infiltration of neutrophils in this model was not dependent on Nalp3/cryopyrin, ASC (apoptosis-associated speck-like protein containing a caspase recruitment domain) or caspase-1 (Figure 2B). These components of the inflammasome complex are key mediators of neutrophil migration in several models of sterile inflammation (21–23).

Interestingly, the accumulation of neutrophils in the peritoneal cavity was largely abolished in the absence of IL-1 receptor type I (IL-1R; Figure 2C). This effect was specific as numbers of Ly6C<sup>hi</sup> monocytes, B lymphocytes, T lymphocytes and dendritic cells in the peritoneal exudate were comparable to wild-type mice. The depletion of neutrophils was evident at 1 day or 2 weeks post-TMPD treatment, indicating that IL-1R signaling mediates both acute and chronic neutrophil recruitment in this model (Figure 2D). Consistent with these findings, morphological analysis of PECs from TMPD treated IL-1R<sup>-/-</sup> mice showed a

predominance of monocytes and lymphocytes whereas few neutrophils were present (Figure 2E). Moreover, expansion of the neutrophil compartment in the peripheral blood also was abrogated in the absence of IL-1R (Figure 2F). These data suggest that neutrophil recruitment in the TMPD model of chronic inflammation is specifically mediated by IL-1R signaling.

### **MyD88 and IL-1R-associated kinases (IRAKs) modulate both monocyte and neutrophil recruitment**

To elucidate the pathway downstream of IL-1R, we tested the effects of TMPD in mice deficient of the adaptor molecules involved in IL-1R signaling including MyD88 and members of the IRAK family (24–26). Consistent with the essential role of MyD88 and IRAK-4 in IL-1R signaling, the number of neutrophils in the peritoneal cavity after TMPD treatment was significantly reduced in the absence of these molecules (Figure 3A). Unlike IL-1R<sup>-/-</sup> mice, which demonstrated normal recruitment of Ly6C<sup>hi</sup> monocytes (Figure 2C), TMPD-treated IRAK-4<sup>-/-</sup> mice exhibited a drastic reduction of these inflammatory monocytes in the peritoneal cavity (Figure 3B). As described previously (15), this also was seen MyD88-deficient mice. In the absence of significant monocyte and neutrophil influx, the total number of PECs was reduced by > 90% in MyD88<sup>-/-</sup> and IRAK-4<sup>-/-</sup> mice compared to wild-type mice (not shown).

IRAK-1 and IRAK-2 differentially regulate the signaling cascade downstream of IRAK-4 (27). Curiously, the recruitment of neutrophils was partially intact in the absence of either of these kinases (Figure 3B). Combined deficiency of IRAK-1 and IRAK-2 was required to recapitulate the observations in IRAK-4<sup>-/-</sup> mice, suggesting that IRAK-1 and IRAK-2 can partially compensate for one another in the inflammatory response to TMPD.

Although the mechanisms of monocyte and neutrophil recruitment both require MyD88 and IRAKs, these pathways can be distinguished by downstream utilization of interferon regulated factor-7 (IRF-7). IRF-7 interacts with MyD88 and IRAKs to promote TLR-induced IFN-I production but does not participate in IL-1R signaling (28, 29). Consistent with requirement of TLR-7 activation and IFN-I production for monocyte recruitment (15, 16), IRF-7 deficiency resulted in defective accumulation of Ly6C<sup>hi</sup> monocytes, but not neutrophils, following TMPD treatment (Figure 3A and B). Taken together, these data suggest that IL-1R signaling specifically mediates neutrophil influx while the adaptor molecule MyD88 and IRAKs 1/2/4 are shared with the pathway utilized for monocyte recruitment.

### **IL-1 $\alpha$ , but not IL-1 $\beta$ is responsible for the influx of neutrophils**

Since the IL-1R mediates responses to both IL-1 $\alpha$  and IL-1 $\beta$ , we next evaluated the role of these cytokines in TMPD-treated mice. Compared to wild-type controls, IL-1 $\beta$ -deficient mice exhibited comparable levels of neutrophil recruitment two weeks after TMPD injection (Figure 4A, B). In line with these findings, the absence of caspase-1, a protease that generates the active form of IL-1 $\beta$ , did not impact the neutrophil response (see Figure 2B). To address the role of IL-1 $\alpha$ , we tested the effects of monoclonal neutralizing antibodies against IL-1 $\alpha$  in mice treated with TMPD. A single dose of anti-IL-1 $\alpha$  antibodies reduced the infiltration of neutrophils by approximately 40–50% (Figure 4C, D). This effect was specific to neutrophils as the numbers of monocytes and lymphocytes in the peritoneal cavity were not affected (data not shown). Therefore, IL-1 $\alpha$  is the primary mediator of neutrophil influx in this model.

## IL-1 $\alpha$ promotes neutrophil recruitment by inducing CXCL5 expression

To further understand the mechanism of neutrophil migration driven by IL-1 $\alpha$ , we studied the involvement of chemokines downstream of IL-1R signaling. Several members of the CXC chemokine family are potent neutrophil chemoattractants produced in response to IL-1R stimulation (30–32). *In vitro* studies using cultured fibroblasts showed that IL-1 $\alpha$  and IL-1 $\beta$  are equally effective in upregulating the transcription of the neutrophil chemoattractants CXCL1 and CXCL5 (supplemental figure 2). In PECs from TMPD-treated mice, expression of the neutrophil chemoattractants CXCL1, CXCL2, CXCL3 and CXCL5 as well as the monocyte chemoattractants CCL2, CCL12 and CX<sub>3</sub>CL1 all were detectable using Q-PCR (Figure 5A). However, the transcript levels of CXCL5 were reduced significantly in IL-1R-deficient mice compared to wild-type controls, whereas the expression other CXC chemokines and monocyte chemoattractants was largely unaffected. Supporting these findings, CXCL5 protein was readily detectable in the peritoneal lavage fluid at 1 day, 2 weeks and 1 month post-TMPD treatment (Figure 5B). CXCL5 levels were drastically reduced in the peritoneal lavage fluid from TMPD-treated IL-1R<sup>-/-</sup> mice (Figure 5C), whereas deficiency of IL-1 $\beta$  did not impact the production of this chemokine. The expression of CXCL5, but not CXCL1, CXCL2 or CXCL3, was similarly reduced by the administration of anti-IL-1 $\alpha$  antibodies (Figure 5D). IL-1 $\alpha$  blockade also reduced CXCL5 protein levels in the peritoneal lavage fluid (Figure 5E).

In contrast to CXCL5, the amounts of CXCL1 in the peritoneal lavage fluid from TMPD-treated mice were small (Figure 5F). Interestingly, although significant amounts of CXCL2 were detected in the lavage fluid, the production of this chemokine is intact in the absence of IL-1 receptor (Figure 5G). Since IL-1 signaling is responsible for about 90% of neutrophil influx both acutely and chronically after TMPD treatment (Figure 2D), CXCL2 is unlikely to be the major neutrophil chemoattractant in this model.

To further evaluate whether CXCL5 is critical to neutrophil migration in this model, we tested the effect of TMPD in mice deficient of CXCR2, the primary receptor for CXCL5. Compared to wild-type BALB/c controls, CXCR2<sup>-/-</sup> mice exhibited ~90% reduction of neutrophil influx to the peritoneal cavity in response to TMPD treatment, recapitulating the observations in IL-1R<sup>-/-</sup> mice (Figure 5H, I). Finally, we investigated the effect of CXCL5 blockade on granulocyte recruitment. Administration of neutralizing antibodies to CXCL5 reduced the infiltration of granulocytes to the peritoneal cavity by about 30% compared to treatment with isotype control antibodies (Figure 5J). Taken together, these data suggest that IL-1 $\alpha$  and IL-1R signaling promotes the chronic infiltration of granulocytes at least in part by inducing CXCL5 expression.

## Discussion

The pro-inflammatory effects of naturally-occurring hydrocarbon oils were described more than a half century ago (7). These properties have been applied to the development of vaccines, in which hydrocarbons are commonly incorporated as adjuvants to augment the response to immunization (6, 7). On the other hand, exposure to hydrocarbons is associated with the development of chronic inflammation and a variety of pathological findings including plasmacytoma formation, lymphoid neogenesis, and autoimmune manifestations (2–5). The mechanism(s) of hydrocarbon-induced inflammation remains largely unexplained.

TMPD is a medium-length hydrocarbon that elicits a potent chronic inflammatory response in mice characterized by persistent infiltration of neutrophils and monocytes (8). In this study, we illustrate the essential role of IL-1 $\alpha$  in TMPD-induced neutrophil recruitment. IL-1 $\alpha$  activates a pathway that requires IL-1R, MyD88, IRAK1/2, and IRAK-4, leading to a

signaling cascade that culminates in the production of the neutrophil chemoattractant CXCL5 (Figure 6). Blockade of IL-1 $\alpha$  reduced the production of CXCL5 and infiltration of neutrophils to the peritoneal cavity in TMPD-treated mice. In contrast, neutrophil influx was not impacted by the absence of other pro-inflammatory mediators including IL-1 $\beta$ , TNF- $\alpha$ , IL-6, and TLR4. Both IFN- $\gamma$  and IFN-I are also dispensable (16). This mechanism is also different from the pathway utilized in chronic monocyte recruitment in the TMPD model (15, 16). The persistent influx of monocytes is mediated by the production of several CC-chemokines downstream of TLR-7 activation and IFN-I production (Figure 6). Interestingly, the IL-1R and TLR signaling cascades share key signaling molecules including MyD88 and IRAK-4 (24–26). As a result, the recruitment of both neutrophils and monocytes is abolished in the absence of these molecules. These pathways diverge downstream of IRAK signaling. IFN-I production and monocyte recruitment initiated by TLR7 depend on the transcription factor IRF-7, whereas IL-1R signaling and neutrophil recruitment is IRF-7 independent and likely mediated by nuclear factor-kappa B (NF- $\kappa$ B) activation(33, 34).

How TMPD triggers the release of IL-1 $\alpha$  remains to be solved. Recent evidence suggests that dying cells and cellular debris from the chronic inflammatory response may contribute to the release of this cytokine. Introduction of necrotic cells to the peritoneal cavity triggers neutrophil migration in an IL-1 $\alpha$ -dependent manner (35). Interestingly, the release of IL-1 $\alpha$  during necrosis, but not apoptosis, distinguishes the inflammatory response to the two types of cell death (36). Furthermore, necrotic cell debris is also a source of RNA-associated autoantigens (such as components of small ribonucleoproteins) (37–39), which may be responsible for the activation of TLR-7 and subsequent recruitment of Ly6C<sup>hi</sup> monocytes in this model (Figure 6). The target(s) of IL-1 $\alpha$  is also not completely understood. Although gene expression data in PECs suggest a role of these inflammatory cells in the production of neutrophil chemoattractants, mesothelial cells also could be a major source of these chemokines. A recent study demonstrates that IL-1 $\alpha$  released from dying cells stimulates the migration of neutrophils by inducing CXCL1 expression by mesothelial cells (40). While a similar mechanism may be involved in TMPD-induced chronic inflammation, CXCL5 rather than CXCL1 seems to play a more prominent role in TMPD-induced neutrophil recruitment. Additional studies will be needed to distinguish the roles of mesothelial cells and PECs in this model.

In addition to modulating chemokine production, IL-1 $\alpha$  and IL-1R signaling possess other functions that may fuel the chronic inflammatory response. Transgenic overexpression of IL-1 $\alpha$  in mice is sufficient to trigger a form of arthritis characterized by a predominance of macrophages and neutrophils in the synovium (41). As TMPD-treated BALB/c mice develop an inflammatory arthritis(42), it will be of interest to examine the effect of IL-1R deficiency on the pathogenesis of arthritis in this model. IL-1 $\alpha$  also is thought to be responsible for the maintenances of granulopoiesis through the induction of neutrophil-macrophage colony-stimulating factor expression (41, 43). Indeed, the proliferation of not only neutrophil/macrophage progenitors, but also multipotent progenitors and hematopoietic stem cells, is supported by IL-1R signaling (44). This chemokine-independent mechanism may be responsible for the peripheral granulocytosis in TMPD-treated mice, although the effects of TMPD on the different progenitor populations have not been assessed.

CXCL5, also known as epithelial cell-derived neutrophil attractant 78 (ENA-78), directs the migration of neutrophils primarily via the receptor CXCR2 (45, 46). The interaction between CXCL5 and CXCR2 is critical for neutrophil recruitment in several models of inflammatory disease (47–50). CXCL5 expression is induced by IL-1 $\alpha$ , IL-1 $\beta$ , and TNF- $\alpha$  through activation of NF- $\kappa$ B(51–54), whereas IFN- $\alpha$  and IFN- $\gamma$  both suppress the production of this chemokine (55, 56). Production of CXCL5 downstream of kinin B1 receptor activation plays an important role in IL-1 $\beta$ -induced neutrophil migration (57).

Interestingly, CXCL5 is also a mediator of neutrophil migration in the inflammatory response induced by IL-23 and IL-17 (58). While our data suggest that IL-1 $\alpha$  is responsible for CXCL5 production in the TMPD-model, whether the IL-23/IL-17 axis modulates IL-1 $\alpha$  or CXCL5 expression warrants further investigation. It is noteworthy that our observations are also distinct from the inflammatory response to turpentine oil, which relies on IL- $\beta$  production (59, 60). Furthermore, the monocyte chemoattractant CCL2 has been implicated in the chronic infiltration of neutrophils in a model adjuvant-induced vasculitis (61). The involvement of CCL2 and its receptor CCR2, however, seems limited to the regulation of monocyte migration in mice exposed to i.p. TMPD.

A potential limitation of the current study is the partial response exhibited by IL-1 $\alpha$  and CXCL5 blockade. Whereas the influx of neutrophils was inhibited by > 90% in IL-1R $^{-/-}$  and CXCR2 $^{-/-}$  mice, neutralization of IL-1 $\alpha$  or CXCL5 only achieved a reduction of 30–40%. This level of response is comparable to another study that administered these antibodies i.p. (35, 58). While the partial response is likely due to the unremitting inflammatory response to TMPD and/or the presence of neutrophils in the peritoneal cavity prior to administration of antibodies, it remains possible that other co-factors are involved. For example, IL-1 signaling can directly activate the vascular endothelium to augment neutrophil chemotaxis(62).

In conclusion, our study elucidates the molecular pathway responsible for neutrophil recruitment in hydrocarbon-induced chronic inflammation. These findings highlight the role of IL-1 $\alpha$  in maintaining persistent neutrophil recruitment to sites of inflammation at least in part by regulating CXCL5 production. In view of the induction of lupus by TMPD, the current data also may be of interest with regard to the recent evidence that proinflammatory neutrophils are involved in the pathogenesis of vascular disease in lupus patients (63). Whether therapeutic interventions targeting IL-1 $\alpha$ , CXCL5 or CXCR2 are effective in chronic inflammatory or vascular diseases or in the inflammatory arthritis induced by TMPD, warrants further evaluation.

## Supplementary Material

Refer to Web version on PubMed Central for supplementary material.

## Acknowledgments

We thank Dr. Vishva Dixit (Genetech, San Francisco, CA) for generously providing ASC $^{-/-}$ , Nalp3 $^{-/-}$ , and caspase-1 $^{-/-}$  mice, Drs. Nicolas Turrin (Laval University, Quebec, Canada), Scott Berceci, and Kerry O'Malley (University of Florida) for generously providing IL-1 $\beta$  $^{-/-}$  mice, M. Kumagai, Y. Fujiwara, and A. Yoshimura for technical assistance, and E. Kamada for secretarial assistance. We also thank the Malcolm Randall VA Medical Center animal facility (Gainesville, FL) for assistance with animal husbandry.

## References

1. Kumar, V.; Abbas, AK.; Fausto, N.; Robbins, SL.; Cotran, RS. Acute and Chronic Inflammation. In: Kumar, V.; Abbas, A.; Fausto, N., editors. Robbins & Cotran Pathologic Basis of Disease. 7. Elsevier Health Sciences; Philadelphia, PA: 2004. p. 50-88.
2. Reeves WH, Lee PY, Weinstein JS, Satoh M, Lu L. Induction of autoimmunity by pristane and other naturally occurring hydrocarbons. Trends Immunol. 2009; 30:455–464. [PubMed: 19699150]
3. Spickard A 3rd, Hirschmann JV. Exogenous lipid pneumonia. Arch Intern Med. 1994; 154:686–692. [PubMed: 8129503]
4. Satoh M, Reeves WH. Induction of lupus-associated autoantibodies in BALB/c mice by intraperitoneal injection of pristane. J Exp Med. 1994; 180:2341–2346. [PubMed: 7964507]



5. Anderson PN, Potter M. Induction of plasma cell tumours in BALB-c mice with 2,6,10,14-tetramethylpentadecane (pristane). *Nature*. 1969; 222:994–995. [PubMed: 5789334]
6. Wilner BI, Evers MA, Troutman HD, Trader FW, McLean IW. Vaccine Potentiation by Emulsification with Pure Hydrocarbon Compounds. *J Immunol*. 1963; 91:210–229. [PubMed: 14061377]
7. Ehrich WE, Halbert SP, Mertens E, Mudd S. Mechanism of the Augmenting Action of Mineral Oil on Antibody Production : Tissue Reactions and Antibody Response to Dysentery Vaccine in Saline, and in Saline-Lanolin-Mineral Oil Emulsion. *J Exp Med*. 1945; 82:343–360. [PubMed: 19871505]
8. Cancro M, Potter M. The requirement of an adherent cell substratum for the growth of developing plasmacytoma cells in vivo. *J Exp Med*. 1976; 144:1554–1567. [PubMed: 1003103]
9. Nacionales DC, Kelly KM, Lee PY, Zhuang H, Li Y, Weinstein JS, Sobel E, Kuroda Y, Akaogi J, Satoh M, Reeves WH. Type I interferon production by tertiary lymphoid tissue developing in response to 2,6,10,14-tetramethyl-pentadecane (pristane). *Am J Pathol*. 2006; 168:1227–1240. [PubMed: 16565497]
10. Patten C, Bush K, Rioja I, Morgan R, Wooley P, Trill J, Life P. Characterization of pristane-induced arthritis, a murine model of chronic disease: response to antirheumatic agents, expression of joint cytokines, and immunopathology. *Arthritis Rheum*. 2004; 50:3334–3345. [PubMed: 15476226]
11. Satoh M, Hamilton KJ, Ajmani AK, Dong X, Wang J, Kanwar YS, Reeves WH. Autoantibodies to ribosomal P antigens with immune complex glomerulonephritis in SJL mice treated with pristane. *J Immunol*. 1996; 157:3200–3206. [PubMed: 8816434]
12. Satoh M, Kumar A, Kanwar YS, Reeves WH. Anti-nuclear antibody production and immune-complex glomerulonephritis in BALB/c mice treated with pristane. *Proc Natl Acad Sci U S A*. 1995; 92:10934–10938. [PubMed: 7479913]
13. Chowdhary VR, Grande JP, Luthra HS, David CS. Characterization of haemorrhagic pulmonary capillaritis: another manifestation of Pristane-induced lupus. *Rheumatology (Oxford)*. 2007; 46:1405–1410. [PubMed: 17576695]
14. Hoogenraad N, Helman T, Hoogenraad J. The effect of pre-injection of mice with pristane on ascites tumour formation and monoclonal antibody production. *J Immunol Methods*. 1983; 61:317–320. [PubMed: 6875258]
15. Lee PY, Kumagai Y, Li Y, Takeuchi O, Yoshida H, Weinstein J, Kellner ES, Nacionales D, Barker T, Kelly-Scumpia K, van Rooijen N, Kumar H, Kawai T, Satoh M, Akira S, Reeves WH. TLR7-dependent and Fc{gamma}R-independent production of type I interferon in experimental mouse lupus. *J Exp Med*. 2008; 205:2995–3006. [PubMed: 19047436]
16. Lee PY, Li Y, Kumagai Y, Xu Y, Weinstein JS, Kellner ES, Nacionales DC, Butfiloski EJ, van Rooijen N, Akira S, Sobel ES, Satoh M, Reeves WH. Type I interferon modulates monocyte recruitment and maturation in chronic inflammation. *Am J Pathol*. 2009; 175:2023–2033. [PubMed: 19808647]
17. Lee PY, Weinstein JS, Nacionales DC, Scumpia PO, Li Y, Butfiloski E, van Rooijen N, Moldawer L, Satoh M, Reeves WH. A novel Type I IFN-producing cell subset in murine lupus. *J Immunol*. 2008; 180:5101–5108. [PubMed: 18354236]
18. Livak KJ, Schmittgen TD. Analysis of relative gene expression data using real-time quantitative PCR and the 2<sup>(-Delta Delta C(T))</sup> Method. *Methods*. 2001; 25:402–408. [PubMed: 11846609]
19. Voehringer D, van Rooijen N, Locksley RM. Eosinophils develop in distinct stages and are recruited to peripheral sites by alternatively activated macrophages. *J Leukoc Biol*. 2007; 81:1434–1444. [PubMed: 17339609]
20. Kuroda Y, Akaogi J, Nacionales DC, Wasdo SC, Szabo NJ, Reeves WH, Satoh M. Distinctive patterns of autoimmune response induced by different types of mineral oil. *Toxicol Sci*. 2004; 78:222–228. [PubMed: 14718649]
21. Franchi L, Eigenbrod T, Munoz-Planillo R, Nunez G. The inflammasome: a caspase-1-activation platform that regulates immune responses and disease pathogenesis. *Nat Immunol*. 2009; 10:241–247. [PubMed: 19221555]

22. Hornung V, Bauernfeind F, Halle A, Samstad EO, Kono H, Rock KL, Fitzgerald KA, Latz E. Silica crystals and aluminum salts activate the NALP3 inflammasome through phagosomal destabilization. *Nat Immunol.* 2008; 9:847–856. [PubMed: 18604214]
23. Martinon F, Petrilli V, Mayor A, Tardivel A, Tschopp J. Gout-associated uric acid crystals activate the NALP3 inflammasome. *Nature.* 2006; 440:237–241. [PubMed: 16407889]
24. Suzuki N, Suzuki S, Duncan GS, Millar DG, Wada T, Mirtsos C, Takada H, Wakeham A, Itie A, Li S, Penninger JM, Wesche H, Ohashi PS, Mak TW, Yeh WC. Severe impairment of interleukin-1 and Toll-like receptor signalling in mice lacking IRAK-4. *Nature.* 2002; 416:750–756. [PubMed: 11923871]
25. Adachi O, Kawai T, Takeda K, Matsumoto M, Tsutsui H, Sakagami M, Nakanishi K, Akira S. Targeted disruption of the MyD88 gene results in loss of IL-1- and IL-18-mediated function. *Immunity.* 1998; 9:143–150. [PubMed: 9697844]
26. Muzio M, Ni J, Feng P, Dixit VM. IRAK (Pelle) family member IRAK-2 and MyD88 as proximal mediators of IL-1 signaling. *Science.* 1997; 278:1612–1615. [PubMed: 9374458]
27. Kawagoe T, Sato S, Matsushita K, Kato H, Matsui K, Kumagai Y, Saitoh T, Kawai T, Takeuchi O, Akira S. Sequential control of Toll-like receptor-dependent responses by IRAK1 and IRAK2. *Nat Immunol.* 2008; 9:684–691. [PubMed: 18438411]
28. Honda K, Yanai H, Negishi H, Asagiri M, Sato M, Mizutani T, Shimada N, Ohba Y, Takaoka A, Yoshida N, Taniguchi T. IRF-7 is the master regulator of type-I interferon-dependent immune responses. *Nature.* 2005; 434:772–777. [PubMed: 15800576]
29. Uematsu S, Sato S, Yamamoto M, Hirohata T, Kato H, Takeshita F, Matsuda M, Coban C, Ishii KJ, Kawai T, Takeuchi O, Akira S. Interleukin-1 receptor-associated kinase-1 plays an essential role for Toll-like receptor (TLR)7- and TLR9-mediated interferon- $\alpha$  induction. *J Exp Med.* 2005; 201:915–923. [PubMed: 15767370]
30. Groves RW, Rauschmayr T, Nakamura K, Sarkar S, Williams IR, Kupper TS. Inflammatory and hyperproliferative skin disease in mice that express elevated levels of the IL-1 receptor (type I) on epidermal keratinocytes. Evidence that IL-1-inducible secondary cytokines produced by keratinocytes in vivo can cause skin disease. *J Clin Invest.* 1996; 98:336–344. [PubMed: 8755642]
31. Tumpey TM, Fenton R, Molesworth-Kenyon S, Oakes JE, Lausch RN. Role for macrophage inflammatory protein 2 (MIP-2), MIP-1 $\alpha$ , and interleukin-1 $\alpha$  in the delayed-type hypersensitivity response to viral antigen. *J Virol.* 2002; 76:8050–8057. [PubMed: 12134010]
32. West-Mays JA, Sadow PM, Tobin TW, Strissel KJ, Cintron C, Fini ME. Repair phenotype in corneal fibroblasts is controlled by an interleukin-1  $\alpha$  autocrine feedback loop. *Invest Ophthalmol Vis Sci.* 1997; 38:1367–1379. [PubMed: 9191600]
33. Dinarello CA. Immunological and inflammatory functions of the interleukin-1 family. *Annu Rev Immunol.* 2009; 27:519–550. [PubMed: 19302047]
34. Leung K, Betts JC, Xu L, Nabel GJ. The cytoplasmic domain of the interleukin-1 receptor is required for nuclear factor- $\kappa$ B signal transduction. *J Biol Chem.* 1994; 269:1579–1582. [PubMed: 8294399]
35. Chen CJ, Kono H, Golenbock D, Reed G, Akira S, Rock KL. Identification of a key pathway required for the sterile inflammatory response triggered by dying cells. *Nat Med.* 2007; 13:851–856. [PubMed: 17572686]
36. Cohen I, Rider P, Carmi Y, Braiman A, Dotan S, White MR, Voronov E, Martin MU, Dinarello CA, Apte RN. Differential release of chromatin-bound IL-1 $\alpha$  discriminates between necrotic and apoptotic cell death by the ability to induce sterile inflammation. *Proc Natl Acad Sci U S A.* 2010; 107:2574–2579. [PubMed: 20133797]
37. Barrat FJ, Meeker T, Gregorio J, Chan JH, Uematsu S, Akira S, Chang B, Duramad O, Coffman RL. Nucleic acids of mammalian origin can act as endogenous ligands for Toll-like receptors and may promote systemic lupus erythematosus. *J Exp Med.* 2005; 202:1131–1139. [PubMed: 16230478]
38. Lau CM, Broughton C, Tabor AS, Akira S, Flavell RA, Mamula MJ, Christensen SR, Shlomchik MJ, Viglianti GA, Rifkin IR, Marshak-Rothstein A. RNA-associated autoantigens activate B cells by combined B cell antigen receptor/Toll-like receptor 7 engagement. *J Exp Med.* 2005; 202:1171–1177. [PubMed: 16260486]

39. Vollmer J, Tluk S, Schmitz C, Hamm S, Jurk M, Forsbach A, Akira S, Kelly KM, Reeves WH, Bauer S, Krieg AM. Immune stimulation mediated by autoantigen binding sites within small nuclear RNAs involves Toll-like receptors 7 and 8. *J Exp Med*. 2005; 202:1575–1585. [PubMed: 16330816]
40. Eigenbrod T, Park JH, Harder J, Iwakura Y, Nunez G. Cutting edge: critical role for mesothelial cells in necrosis-induced inflammation through the recognition of IL-1 alpha released from dying cells. *J Immunol*. 2008; 181:8194–8198. [PubMed: 19050234]
41. Niki Y, Yamada H, Seki S, Kikuchi T, Takaishi H, Toyama Y, Fujikawa K, Tada N. Macrophage- and neutrophil-dominant arthritis in human IL-1 alpha transgenic mice. *J Clin Invest*. 2001; 107:1127–1135. [PubMed: 11342576]
42. Potter M, Wax JS. Genetics of susceptibility to pristane-induced plasmacytomas in BALB/cAn: reduced susceptibility in BALB/cJ with a brief description of pristane-induced arthritis. *J Immunol*. 1981; 127:1591–1595. [PubMed: 7276572]
43. Stork LC V, Peterson M, Rundus CH, Robinson WA. Interleukin-1 enhances murine granulopoiesis in vivo. *Exp Hematol*. 1988; 16:163–167. [PubMed: 3257444]
44. Ueda Y, Cain DW, Kuraoka M, Kondo M, Kelsoe G. IL-1R type I-dependent hemopoietic stem cell proliferation is necessary for inflammatory granulopoiesis and reactive neutrophilia. *J Immunol*. 2009; 182:6477–6484. [PubMed: 19414802]
45. Corbett MS, Schmitt I, Riess O, Walz A. Characterization of the gene for human neutrophil-activating peptide 78 (ENA-78). *Biochem Biophys Res Commun*. 1994; 205:612–617. [PubMed: 7999089]
46. Walz A, Burgener R, Car B, Baggiolini M, Kunkel SL, Strieter RM. Structure and neutrophil-activating properties of a novel inflammatory peptide (ENA-78) with homology to interleukin 8. *J Exp Med*. 1991; 174:1355–1362. [PubMed: 1744577]
47. Grespan R, Fukada SY, Lemos HP, Vieira SM, Napimoga MH, Teixeira MM, Fraser AR, Liew FY, McInnes IB, Cunha FQ. CXCR2-specific chemokines mediate leukotriene B4-dependent recruitment of neutrophils to inflamed joints in mice with antigen-induced arthritis. *Arthritis Rheum*. 2008; 58:2030–2040. [PubMed: 18576322]
48. Halloran MM, Woods JM, Strieter RM, Szekanecz Z, Volin MV, Hosaka S, Haines GK 3rd, Kunkel SL, Burdick MD, Walz A, Koch AE. The role of an epithelial neutrophil-activating peptide-78-like protein in rat adjuvant-induced arthritis. *J Immunol*. 1999; 162:7492–7500. [PubMed: 10358204]
49. Colletti LM, Kunkel SL, Walz A, Burdick MD, Kunkel RG, Wilke CA, Strieter RM. Chemokine expression during hepatic ischemia/reperfusion-induced lung injury in the rat. The role of epithelial neutrophil activating protein. *J Clin Invest*. 1995; 95:134–141. [PubMed: 7814607]
50. Koch AE, Kunkel SL, Harlow LA, Mazarakis DD, Haines GK, Burdick MD, Pope RM, Walz A, Strieter RM. Epithelial neutrophil activating peptide-78: a novel chemotactic cytokine for neutrophils in arthritis. *J Clin Invest*. 1994; 94:1012–1018. [PubMed: 8083342]
51. Fillmore RA, Nelson SE, Lausch RN, Oakes JE. Differential regulation of ENA-78 and GCP-2 gene expression in human corneal keratocytes and epithelial cells. *Invest Ophthalmol Vis Sci*. 2003; 44:3432–3437. [PubMed: 12882792]
52. Chang MS, McNinch J, Basu R, Simonet S. Cloning and characterization of the human neutrophil-activating peptide (ENA-78) gene. *J Biol Chem*. 1994; 269:25277–25282. [PubMed: 7929219]
53. Lee YR, Kweon SH, Kwon KB, Park JW, Yoon TR, Park BH. Inhibition of IL-1beta-mediated inflammatory responses by the IkappaB alpha super-repressor in human fibroblast-like synoviocytes. *Biochem Biophys Res Commun*. 2009; 378:90–94. [PubMed: 19007749]
54. Madorin WS, Rui T, Sugimoto N, Handa O, Cepinskas G, Kvietys PR. Cardiac myocytes activated by septic plasma promote neutrophil transendothelial migration: role of platelet-activating factor and the chemokines LIX and KC. *Circ Res*. 2004; 94:944–951. [PubMed: 14988231]
55. Wuyts A, Struyf S, Gijssbers K, Schutyser E, Put W, Conings R, Lenaerts JP, Geboes K, Opdenakker G, Menten P, Proost P, Van Damme J. The CXC chemokine GCP-2/CXCL6 is predominantly induced in mesenchymal cells by interleukin-1beta and is down-regulated by interferon-gamma: comparison with interleukin-8/CXCL8. *Lab Invest*. 2003; 83:23–34. [PubMed: 12533683]

56. Schnyder-Candrian S, Strieter RM, Kunkel SL, Walz A. Interferon-alpha and interferon-gamma down-regulate the production of interleukin-8 and ENA-78 in human monocytes. *J Leukoc Biol.* 1995; 57:929–935. [PubMed: 7790776]
57. Duchene J, Lecomte F, Ahmed S, Cayla C, Pesquero J, Bader M, Perretti M, Ahluwalia A. A novel inflammatory pathway involved in leukocyte recruitment: role for the kinin B1 receptor and the chemokine CXCL5. *J Immunol.* 2007; 179:4849–4856. [PubMed: 17878384]
58. Lemos HP, Grespan R, Vieira SM, Cunha TM, Verri WA Jr, Fernandes KS, Souto FO, McInnes IB, Ferreira SH, Liew FY, Cunha FQ. Prostaglandin mediates IL-23/IL-17-induced neutrophil migration in inflammation by inhibiting IL-12 and IFN $\gamma$  production. *Proc Natl Acad Sci U S A.* 2009; 106:5954–5959. [PubMed: 19289819]
59. Horai R, Asano M, Sudo K, Kanuka H, Suzuki M, Nishihara M, Takahashi M, Iwakura Y. Production of mice deficient in genes for interleukin (IL)-1 $\alpha$ , IL-1 $\beta$ , IL-1 $\alpha/\beta$ , and IL-1 receptor antagonist shows that IL-1 $\beta$  is crucial in turpentine-induced fever development and glucocorticoid secretion. *J Exp Med.* 1998; 187:1463–1475. [PubMed: 9565638]
60. Zheng H, Fletcher D, Kozak W, Jiang M, Hofmann KJ, Conn CA, Soszynski D, Grabiec C, Trumbauer ME, Shaw A, et al. Resistance to fever induction and impaired acute-phase response in interleukin-1 beta-deficient mice. *Immunity.* 1995; 3:9–19. [PubMed: 7621081]
61. Johnston B, Burns AR, Suematsu M, Issekutz TB, Woodman RC, Kubes P. Chronic inflammation upregulates chemokine receptors and induces neutrophil migration to monocyte chemoattractant protein-1. *J Clin Invest.* 1999; 103:1269–1276. [PubMed: 10225970]
62. Furie MB, McHugh DD. Migration of neutrophils across endothelial monolayers is stimulated by treatment of the monolayers with interleukin-1 or tumor necrosis factor-alpha. *J Immunol.* 1989; 143:3309–3317. [PubMed: 2553810]
63. Denny MF, Yalavarthi S, Zhao W, Thacker SG, Anderson M, Sandy AR, McCune WJ, Kaplan MJ. A distinct subset of proinflammatory neutrophils isolated from patients with systemic lupus erythematosus induces vascular damage and synthesizes type I IFNs. *J Immunol.* 2010; 184:3284–3297. [PubMed: 20164424]

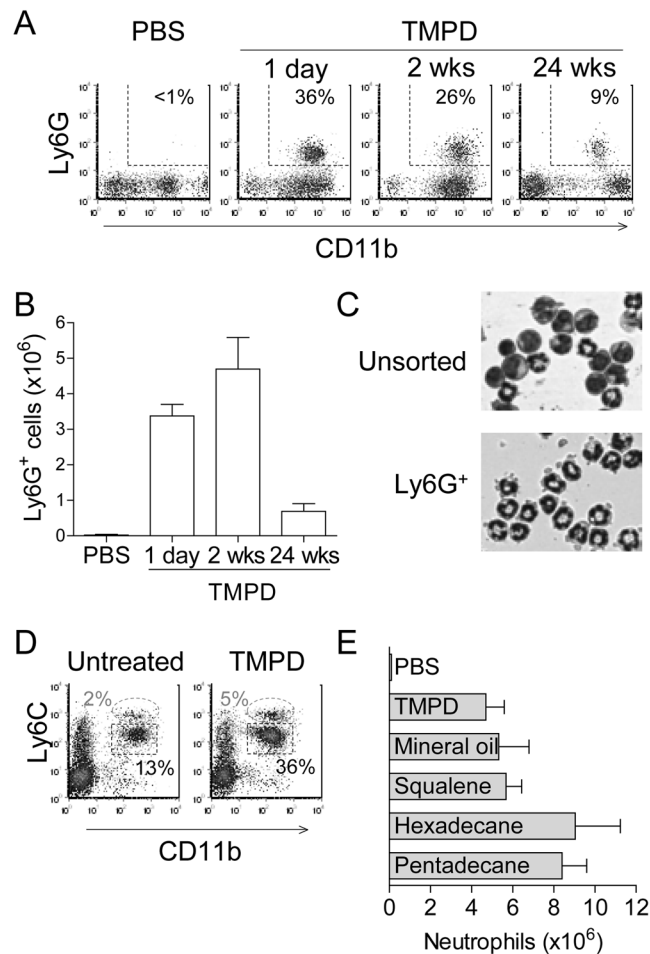


**Figure 1. TMPD induces chronic recruitment of neutrophils in mice**

**A)** Flow cytometry and **B)** quantification of peritoneal exudate cells (PECs) in wild-type C57BL/6 mice treated with PBS or TMPD at the indicated time-points after treatment ( $n = 4$  per group). Neutrophils are characterized by co-expression of CD11b and Ly6G. The percentage of neutrophils is indicated within each plot. **C)** Morphologic analysis of PECs from TMPD-treated mice before and after magnetic bead sorting using anti-Ly6G antibodies (200x magnification). **D)** Flow cytometry of peripheral blood cells in C57BL/6 mice before and two weeks after TMPD treatment. Dotted ovals indicate Ly6C<sup>hi</sup> monocytes (CD11b<sup>+</sup> Ly6C<sup>hi</sup>) and boxes indicate neutrophils (CD11b<sup>+</sup> Ly6C<sup>mid</sup>). The percentage of both populations is indicated within each plot. **E)** Quantification of PECs in C57BL/6 mice treated with PBS or various hydrocarbon oils for two weeks ( $n = 4$  per group). For bar graphs, each bar represents the mean and error bars indicate SE.

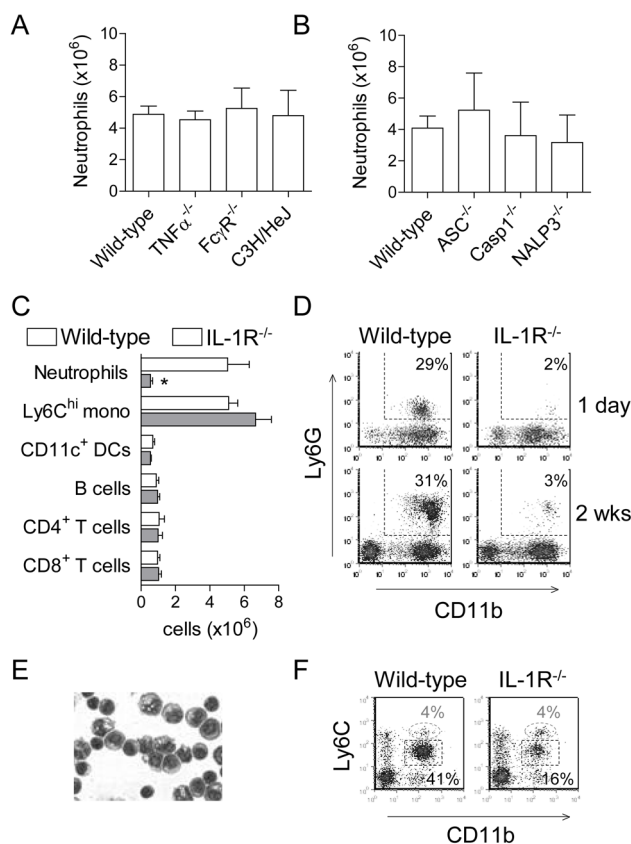


**Figure 2. TMPD-induced neutrophil recruitment is mediated by IL-1R signaling**

**A)** Quantification of Ly6G<sup>+</sup> neutrophils in PECs from TMPD-treated wild-type C57BL/6, TNF- $\alpha$ <sup>-/-</sup>, Fc $\gamma$ -chain<sup>-/-</sup>, and C3H/HeJ mice (n = 6–7 per group). **B)** Quantification of Ly6G<sup>+</sup> neutrophils in PECs from TMPD-treated C57BL/6, ASC<sup>-/-</sup>, caspase-1<sup>-/-</sup>, and NALP3<sup>-/-</sup> mice (n = 8 per group). **C)** Comparison of PEC populations in TMPD-treated C57BL/6 and IL-1R<sup>-/-</sup> mice (n = 6 per group). **D)** Flow cytometry of PECs from C57BL/6 and IL-1R<sup>-/-</sup> mice 1 day or 2 weeks after TMPD treatment. The percentage of neutrophils is indicated within each plot. **E)** Morphologic analysis of PECs from TMPD-treated IL-1R<sup>-/-</sup> mice ( $\times 200$  magnification). **F)** Flow cytometry of peripheral blood cells in TMPD-treated C57BL/6 and IL-1R<sup>-/-</sup> mice. Dotted ovals indicate Ly6C<sup>hi</sup> monocytes (CD11b<sup>+</sup> Ly6C<sup>hi</sup>) and boxes indicate neutrophils (CD11b<sup>+</sup> Ly6C<sup>mid</sup>). The percentages of cells in these populations are indicated within each plot. For all panels, unless otherwise noted, all mice were treated with TMPD 2 weeks prior to analysis. Each bar in bar graphs represents the mean and error bars indicate SE. \* indicates p < 0.05 compared to wild-type controls (Student's unpaired t-test).

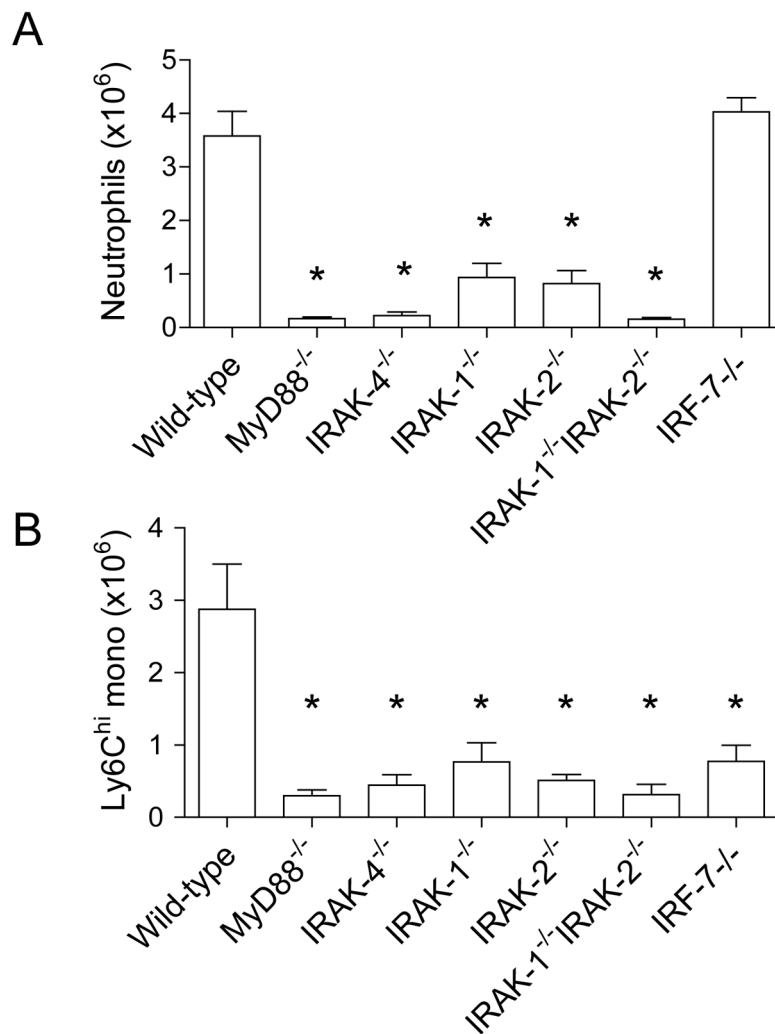


**Figure 3. MyD88 and IRAK-4 mediate the recruitment of both neutrophils and inflammatory monocytes induced by TMPD**

Quantification of A) neutrophils and B) Ly6C<sup>hi</sup> monocytes in PECs from wild-type C57BL/6 (n = 7), MyD88<sup>-/-</sup> (n = 6), IRAK-4<sup>-/-</sup> (n = 8), IRAK-1<sup>-/-</sup> (n = 8), IRAK-2<sup>-/-</sup> (n = 8), IRAK-1<sup>-/-</sup> IRAK-2<sup>-/-</sup> (n = 6), and IRF-7<sup>-/-</sup> (n = 9) mice 2 weeks after TMPD treatment. Each bar represents the mean and error bars indicate SE. \* indicates p < 0.05 compared to wild-type controls (Student's unpaired t-test).

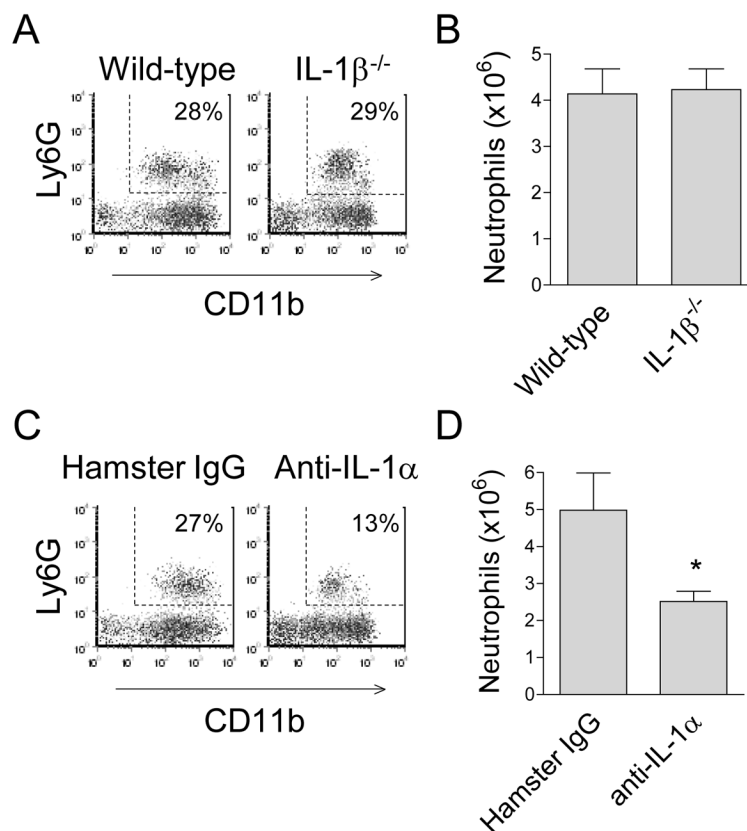


**Figure 4. TMPD-induced neutrophil recruitment requires IL-1 $\alpha$ , but not IL-1 $\beta$**

**A)** Flow cytometry and **B)** Quantification of neutrophils in wild-type C57BL/6 and IL-1 $\beta^{-/-}$  mice two weeks after TMPD treatment ( $n = 7$  per group). **C)** Flow cytometry and **D)** Quantification of neutrophils in C57BL/6 mice injected with 200  $\mu\text{g}$  of hamster IgG or anti-IL-1 $\alpha$  antibodies two weeks after TMPD treatment ( $n = 5$  per group). Analysis was performed 24 hrs after antibody treatment. For all flow cytometry plots, the percentage of neutrophils is indicated within each plot. Each bar in bar graphs represents the mean and error bars indicate SE. \* indicates  $p < 0.05$  compared to wild-type or isotype controls (Student's unpaired t-test).



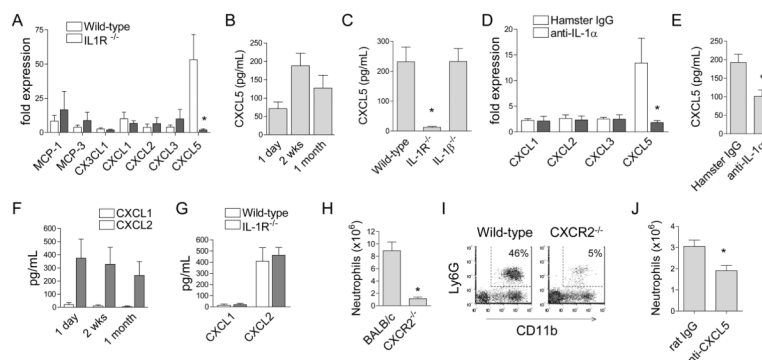


**Figure 5. IL-1 $\alpha$  regulates neutrophil migration by inducing expression of CXCL5 in TMPD-treated mice**

**A)** Q-PCR analysis of chemokine expression in PECs from TMPD-treated C57BL/6 ( $n = 5$ ) and IL-1R<sup>-/-</sup> mice ( $n = 6$ ). ELISA quantification of CXCL5 in peritoneal lavage fluid from **B)** C57BL/6 mice treated with TMPD for the indicated duration ( $n = 4$  to  $5$  per group) and **C)** C57BL/6 ( $n = 5$ ), IL-1R<sup>-/-</sup> ( $n = 6$ ) and IL-1 $\beta$ <sup>-/-</sup> mice ( $n = 4$ ) two weeks after TMPD treatment. **D)** Q-PCR analysis of chemokine expression in PECs from TMPD-treated wild-type C57BL/6 mice injected with 200  $\mu$ g of hamster IgG or anti-IL-1 $\alpha$  antibodies ( $n = 5$  per group). **E)** ELISA quantification of CXCL5 in peritoneal lavage fluid from TMPD-treated C57BL/6 mice injected with hamster IgG or anti-IL-1 $\alpha$  antibodies ( $n = 5$  per group). ELISA quantification of CXCL1 and CXCL2 in peritoneal lavage fluid from **F)** C57BL/6 mice treated with TMPD for the indicated duration ( $n = 4$  to  $5$  per group) and **G)** C57BL/6 ( $n = 5$ ) and IL-1R<sup>-/-</sup> ( $n = 6$ ) two weeks after TMPD treatment. **H)** Quantification and **I)** flow cytometry analysis of neutrophils in wild-type BALB/c and CXCR2<sup>-/-</sup> mice after TMPD treatment ( $n = 7$  per group). **J)** Quantification of neutrophils in C57BL/6 mice injected with 200  $\mu$ g of anti-CXCL5 antibodies or isotype control IgG1 two weeks after TMPD treatment ( $n = 5$  per group). Unless otherwise indicated, all mice were treated with TMPD 2 weeks prior to analysis. Each bar represents the mean and error bars indicate SE. \* indicates  $p < 0.05$  compared to wild-type or isotype controls (Student's unpaired t-test).

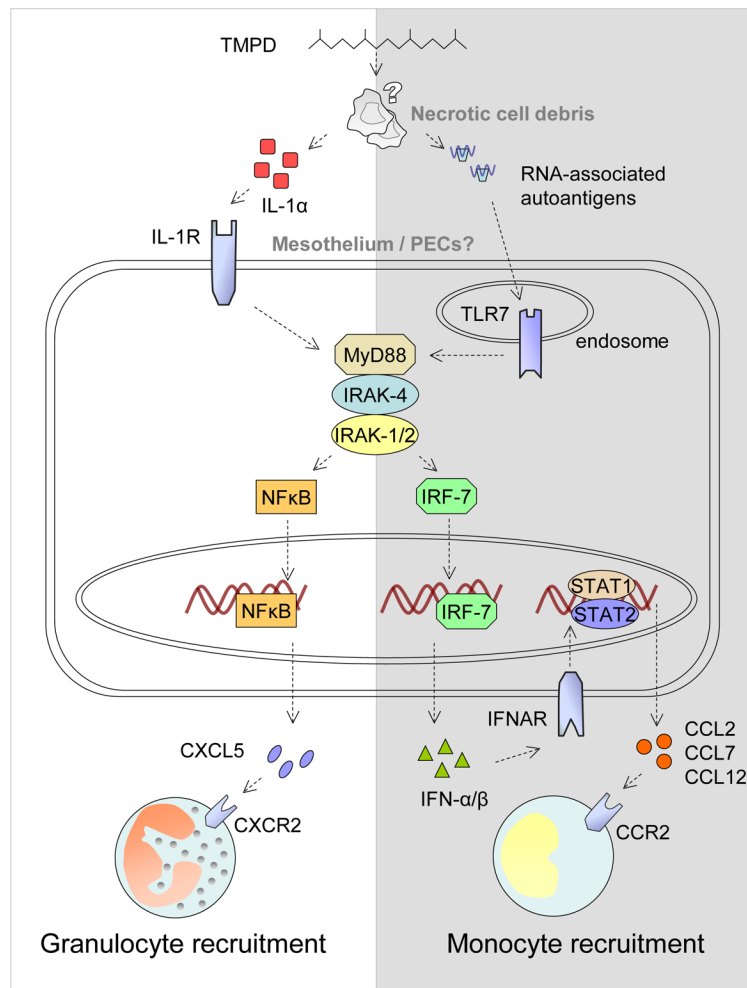


**Figure 6. Proposed pathways of neutrophil and monocyte recruitment in TMPD-induced chronic inflammation**

Neutrophil pathway (left side): TMPD treatment results in the release of IL-1 $\alpha$ , likely from necrotic cells. In target cells such as mesothelial cells or peritoneal exudate cells, IL-1 $\alpha$  stimulates the IL-1R complex, which initiates a signaling cascade that requires MyD88 and IRAKs, culminating in the activation of NF $\kappa$ B and production of the neutrophil chemoattractant CXCL5. Neutrophils migrate to CXCL5 via a CXCR2-dependent mechanism. Monocyte pathway (right side): TMPD treatment results in the activation of TLR-7, which elicits the production of IFN-I through a MyD88-and IRAK-4-dependent pathway. IFN-I binds to IFNAR and subsequent signaling events result in the production of IFN-stimulated chemokines including CCL2, CCL7 and CCL2. These chemokines mediate the migration of Ly6C<sup>hi</sup> monocytes through their interaction with CCR2.

Table 1

Quantification of peritoneal exudate cells in wild-type mouse strains two weeks after TMPD treatment<sup>\*,†</sup>

strain	n	Neutrophils	Ly6C <sup>hi</sup> monocytes	Dendritic cells	B cells	CD4 <sup>+</sup> T cells	CD8 <sup>+</sup> T cells
C57BL/6	6	4.32 ± 0.60	4.80 ± 0.87	0.50 ± 0.07	0.85 ± 0.23	0.90 ± 0.27	0.90 ± 0.23
BALB/cJ	6	9.49 ± 0.43	2.36 ± 0.15	0.23 ± 0.02	0.68 ± 0.05	0.64 ± 0.11	1.13 ± 0.18
129/Sv	6	3.23 ± 0.54	4.85 ± 0.48	0.31 ± 0.08	0.84 ± 0.20	1.03 ± 0.17	0.79 ± 0.14
C3H/OuJ	6	4.80 ± 1.60	4.40 ± 1.53	0.34 ± 0.09	0.80 ± 0.29	0.32 ± 0.08	0.28 ± 0.05
CBA/CaJ	4	3.37 ± 0.38	3.65 ± 1.04	0.27 ± 0.07	0.83 ± 0.24	1.20 ± 0.15	0.37 ± 0.03

\* all values represent cell number X 10<sup>6</sup>

† Cell populations were quantified by flow cytometry using the following surface markers: Neutrophils (CD11b<sup>+</sup>Ly6G<sup>+</sup>), Ly6C<sup>hi</sup> monocytes (CD11b<sup>+</sup>Ly6C<sup>hi</sup>), dendritic cells (CD11C<sup>+</sup>IA/E<sup>+</sup>), B lymphocytes (B220<sup>+</sup>CD11C<sup>-</sup>), CD4<sup>+</sup> T cells (CD4<sup>+</sup>CD11C<sup>-</sup>CD11b<sup>-</sup>) and CD8<sup>+</sup> T cells (CD8<sup>+</sup>CD11C<sup>-</sup>CD11b<sup>-</sup>).